ELSEVIER

Journal of Chromatography A, 829 (1998) 41–63

JOURNAL OF CHROMATOGRAPHY A

Application of the phenomenological model to retention in reversed-phase high-performance liquid chromatography

Jason M. LePree[1,*], Marcella E. Cancino

Arnold and Marie Schwartz College of Pharmacy and Health Sciences, 75 Dekalb Ave., Brooklyn, NY 11201, USA

Received 20 April 1998; received in revised form 10 August 1998; accepted 8 September 1998

Abstract

RP-HPLC, though a widely used and powerful tool for chemical separations, suffers a disadvantage, namely that selection of chromatographic conditions to obtain optimal separation is still often an 'art' rather than science. To remedy this situation and improve our understanding of why retention changes with alterations in mobile phase composition, our laboratory applied the Phenomenological Model of solvent effects to retention data in RP-HPLC for the first time and obtained highly promising results. Specifically, fits to the data were good over a large range of organic solvent concentrations and more importantly, values for the model's adjustable parameters, namely a curvature-corrected molecular surface area term and solvation exchange constants were physically significant.

Keywords: Retention models; Phenomenological model

1. Introduction

RP-HPLC is a widely used and powerful tool for chemical separations and analysis. Unfortunately, ideal separations are often achieved only after optimization of chromatographic method parameters through costly trial-and-error. The problem has generated much research intended to elucidate the mechanism for retention and develop models that relate retention to mobile phase composition, an important chromatographic parameter. Much of this work has been reviewed [1,2]; however, a brief discussion of such work is warranted, particularly work related to the Phenomenological Model of solvent effects discussed in this paper. Three of the equations discussed in the recent reviews take the form of:

$$\ln k' = a + mC \quad (1)$$

where C is either the volume fraction of organic solvent in the mobile phase [3], the E_T30 value of the mobile phase [4,5], or the logarithm of the molar concentration of the organic solvent in the mobile phase [6]. Though simple, these equations cannot describe retention data over an extended cosolvent concentration range because $\ln k'$ is not truly a linear function of C.

Another popular model, based on regular solution theory of solubility, takes the form of Eq. (2):

$$\ln k' = A\varphi^2 + B\varphi + C \quad (2)$$

where A, B, and C are adjustable parameters whose

*Corresponding author. Tel.: +1-203-791-6074; e-mail address: jlepree@bi-pharm.com

[1] Present address: Boehringer Ingelheim Pharmaceuticals, Inc., 900 Ridgebury Rd., P.O. Box 0368, Ridgefield, CT 06877-0368, USA.

0021-9673/98/$ – see front matter
PII: S0021-9673(98)00753-5

values are functions of the molar volume of the solute and the solubility parameters of the solute, the mobile phase, and the stationary phase [7–11]. The model can fit data over extended ranges of organic solvent composition (100% organic to as low as 10% organic solvent) in aqueous–organic binary solvent mixtures and can be extended to describe ternary systems. However, as discussed by Carr and co-workers [12], regular solution theory assumes that the excess entropy and volume of mixing in the solution are zero, and that solute–solvent interactions are equal to the geometric mean of solvent–solvent and solute–solute interactions. These assumptions are not justifiable in the aqueous–organic mobile phases typically used in RP-HPLC, and the lack of actual physical significance in the estimates for *A*, *B*, and *C* may be attributable to the model's improper use in such systems.

Schoenmakers and co-workers [9] have extended the solubility parameter model to account for the dependence of stationary phase polarity on mobile phase composition. This more sophisticated model contains four adjustable parameters and, as anticipated, it can fit retention data over a greater composition range than the three parameter model. However, the limitations of Eq. (2) still apply to the more sophisticated model. Moreover, the parameter estimates are still unrelated to the physical chemical parameters they were intended to represent.

The solvophobic and partition models, discussed next, possess some important similarities to the Phenomenological Model discussed in this paper. Horváth applied solvophobic theory [13,14] to retention in RP-HPLC and developed the solvophobic theory of RP-HPLC [15,16]. According to this pioneering theory, retention is controlled primarily by the energetic cost of creating a cavity in mobile phase to house a solute; the expenditure of energy scales with the microscopic surface tension of the mobile phase and the molecular surface area of the solute. The model played an important role in the early development of mechanistic theory and accounts for two important observations: increases in the surface tension of the mobile phase result in increases in retention, and solutes of larger surface area are retained longer than solutes possessing smaller surface areas. The model has been criticized [17,18] because it doesn't account for observed stationary phase effects on retention, but Horváth and co-workers have responded to such criticisms in a recent publication. In this work [19], the solvophobic theory provided a means to deconvolute retention energetics into contributions from the mobile phase and stationary phase. The results indicated that the mobile phase contribution to retention varied much more with alternations in mobile phase composition than did the stationary phase contribution with changes in hydrocarbon chain length. From these results, Horváth and co-workers concluded that the mobile phase plays the dominant role in controlling retention.

Unlike the solvophobic model, Dill's partition model does account for stationary phase effects on retention [17,18]. According to this theory, retention occurs through a three-step mechanism depicted, with great simplicity, in Fig. 1, where a cavity is created in the stationary phase, the solute is transferred from the mobile phase to the cavity in the stationary phase, and finally the cavity in the mobile phase that once housed the solute is closed. The energetics of the solvent–solvent and solvent–solute interactions of these processes are described through binary interaction constants, and retention is controlled by the differences in these energies. This mechanism has been called a 'partition mechanism'

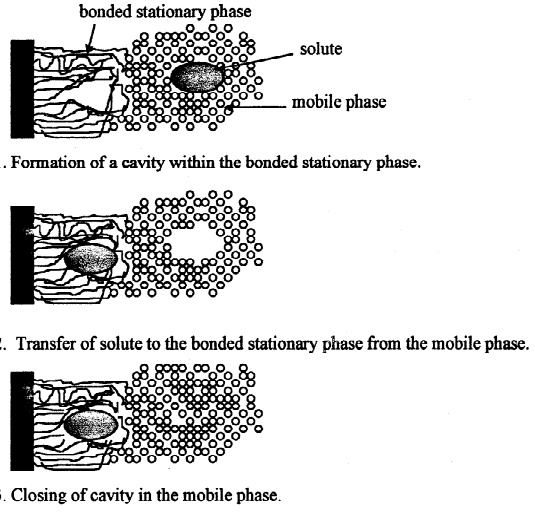

Fig. 1. Mechanism of retention according to the partition theory of Dill [17,18].

because the solute is completely embedded within the stationary phase hydrocarbon chains; a partition mechanism is distinguished from an 'adsorption mechanism' in which the solute is believed to remain only on the surface of the stationary phase chains [17,18,20].

The validity of the partition mechanism will be discussed in subsequent sections; however, it should be noted here that the partition model predicts that retention of a solute, under given chromatographic conditions, will increase with increases in chain density (number of chains/area of solid support) until at sufficiently high chain densities, entropic expulsion of the solute will result leading to decreases in retention. Sentell and Dorsey [20], through well designed experiments, confirmed this prediction and quite convincingly validated the theory. Overall, Dill's model has helped shape the current view of retention mechanisms in RP-HPLC.

Though seemingly different, the solvophobic, solubility parameter, and partition models possess some important similarities. They all describe solvent–solvent interactions through a cavity model and predict that retention will increase with increases in solute size. (Synder's linear solvent strength [2,3] equation predicts that retention will increase with increases in solute size). Furthermore, the solubility parameter and partition models account for solvent–solute interactions and solvent–solvent interactions in both the mobile and stationary phases.

Recently, the Phenomenological Model [21–29] has been used to quantitatively describe solvent effects on a variety of chemical processes in binary aqueous–organic cosolvent systems. Similar to the pioneering models described above, it accounts for solvent–solvent interactions (through a cavity model) and for solute–solvent interactions in the investigated system. The model has been shown to describe solvent effect data over large ranges in solvent composition, and the parameter estimates of the model, obtained by fitting the model to experimental data, appear to possess physically significant values. These characteristics suggest that the Phenomenological Model could provide a useful alternative to the partition, solvophobic, and the solubility parameter models for the description of retention as a function of mobile phase composition. To test its utility, our laboratory adapted the model to describe retention in RP-HPLC and applied it for the first time to retention data from our laboratory and the literature. Our findings indicate that the model can quantitatively describe retention of various solutes over a large range of solvent concentrations in binary organic–water mobile phases. Furthermore, the parameter estimates in the model, namely a term related to the molecular surface area of the investigated solutes is directly proportional to the molecular surface area of the solutes and the solvation exchange constant parameters seem to vary in a physically reasonable manner.

1.1. Theory

A brief review of the model is presented so that the reader can appreciate the model's extension to retention in RP-HPLC. In general, the observed solvent effect is modeled as the sum of contributions from solute–solute interactions (the Intersolute Effect), solvent–solute interactions (the Solvation Effect), and solvent–solvent interactions (the General Medium Effect). For application of the model to retention in RP-HPLC, only the Solvation and General Medium Effects will be considered. A detailed derivation of the model has been presented in the literature [21]; however, in that work and in all past work, the Phenomenological Model was derived to relate the observed solvent effect on the investigated process (complexation, solubility, etc.) to water, the reference solvent [21–29]. To apply the Phenomenological Model to these data, the investigated chemical process was studied in a fully aqueous system, and then in various aqueous–organic binary solvent mixtures. For this study, water cannot be used as a reference solvent because it lacks sufficient solvent strength to elute non-polar compounds from RP-HPLC columns. Therefore in this work, the fully organic system was used as the reference. In earlier unrelated work, Khossravi had derived expressions for the General Medium and Solvation Effects using the fully organic system as the reference [30]. Because the pure organic system is used as the reference, the expressions for the Solvation and General Medium Effects presented below will differ slightly from those previously reported [21–29], though their derivations are similar.

1.1.1. Free energy of partition

The standard free energy change per molecule for the partitioning of a solute from the mobile phase into the stationary phase, ΔG^0_{part}, is given by Eq. (3). (Some workers call this a transfer free energy).

$$\Delta G^0_{part} = -k_B T \ln K = -k_B T \ln\left(\frac{a_s}{a_m}\right) = -k_B T \ln\left(\frac{c_s \gamma_s}{c_m \gamma_m}\right) \quad (3)$$

Here $k_B T$ is the product of the Boltzmann constant and the absolute temperature, K is the thermodynamic equilibrium constant for the partitioning process of a solute from the mobile phase to the stationary phase, a is the activity, c is the molar concentration, γ is the activity coefficient, and the subscripts s and m denote the stationary phase and mobile phase respectively. The standard state is assumed to be the hypothetical one-molar solution, more specifically, a state that a one-molar solution would have if it obeyed Henry's law [31]. We will assume that our chromatography is performed within a concentration range where Henry's law will be obeyed. (This assumption is justified based on the low experimental concentrations used in this work and the good symmetry of our peaks). In this work, we will study the solvent effects on ΔG^*_{part} which is given by Eq. (4). (ΔG^*_{part} will be called an apparent free energy for the partition process).

$$\Delta G^*_{part} = -k_B T \ln K_{app} = -k_B T \ln\left(\frac{c_s}{c_m}\right) \quad (4)$$

Here, K_{app} is an apparent equilibrium constant as it calculated from concentrations rather than activities. (Karger, Synder and Horvath [32] have called K_{app} the distribution constant. Maskill [33] has called it a practical equilibrium constant because it is calculated from concentrations which are accessible from most experimental measurements whereas activities are not. It follows that ΔG°_{part} and ΔG^*_{part} are related by Eq. (5) where all terms have been previously defined. The rightmost term in Eq. (5) is called the excess free energy.

$$\Delta G^*_{part} = \Delta G^0_{part} + k_B T \ln\left(\frac{\gamma_s}{\gamma_m}\right) \quad (5)$$

In this paper, we will not attempt to measure or assume values for the activities or the activity coefficients of the investigated solutes in the stationary phase or the mobile phase, but to develop an explicit phenomenological model for ΔG^*_{part} as a function of the mole fraction concentrations of organic solvent and water in the mobile phase. (LePree, Connors and Mulski [23] used a similar approach to apply the Phenomenological Model to solubility data for naphthalene and 4-nitroaniline in binary aqueous–organic solvent systems. In this work, ΔG^*_{soln}, rather than the standard free energy of solution, was expressed as a function of solvent composition, where $\Delta G^*_{soln} = -k_B T \ln\{\text{mole fraction of solute}\}$ [23].

1.1.2. Solvation effect

The Solvation Effect is modeled as a competitive, stepwise, solvation exchange equilibrium where water (W) competes with an organic solvent molecule (M) to solvate a solute (R) as shown in Scheme 1.

Each step in Scheme 1 is described by a solvation exchange constant denoted as K_n where n refers to the n^{th} step in the process. The solvation exchange constants are apparent equilibrium constants rather than true thermodynamic constants as they are calculated from concentrations instead of activities. Though the model allows for generalization to any number of steps from one to infinity, this paper will make use of the two-step process illustrated in Scheme 2.

Though the equilibria in Scheme 2 is depicted on an individual molecular exchange basis for mathematical convenience, a more chemically defensible view is that the solute exists in three states, namely as a fully solvated, a partially solvated, and a fully

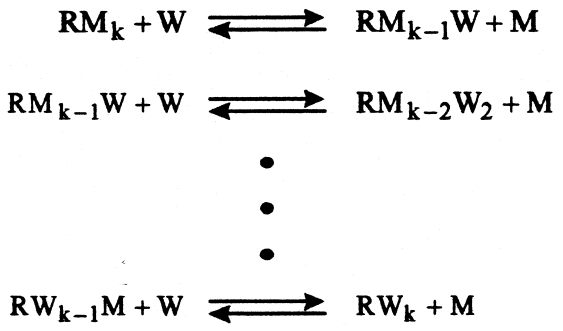

Scheme 1.

$$RM_2 + W \underset{}{\overset{K_1}{\rightleftharpoons}} RMW + M$$

$$RMW + W \underset{}{\overset{K_2}{\rightleftharpoons}} RW_2 + M$$

Scheme 2.

hydrated state. (In general, there are $n+1$ solvation states for every n solvation steps in the model).

It is acknowledged that this is a *great* simplification of the processes that may occur in aqueous–organic solutions. A more accurate depiction requires knowledge of all possible solvated and hydrated states in solution and a knowledge of the structure of liquid water in the presence of non-polar and semi-polar solutes. Although such knowledge is very difficult if not impossible to acquire, it has been the focus of much research work. It is beyond the scope of this paper to review the vast quantity of literature within this field, but the work of Scott and co-workers [34,35] and Guillaume and Guinchard [36] warrants a brief discussion.

Scott and co-workers [34,35] fit data for the volume change on mixing, the density, and the refractive index of methanol–water mixtures to a model which assumed the existence of a three-state system in methanol–water mixtures consisting of water, methanol, and methanol–water associated complexes. They estimated that the concentration of the associated methanol–water complex was as high as 60% (v/v). The extent that the associated water–methanol complex would solvate a solute depended on the solute's polarity. For non-polar solutes like benzene, they concluded that no interaction with the methanol–water complex would occur, but for semi-polar solutes, like 1-pentanol, the interaction would become more important, though solvation by free methanol was still most important. Recently, Guillaume and Guinchard [36] developed a three-state model consisting of solute solvation/hydration by methanol, water, and associated methanol–water. Their model, which related the capacity factor of a solute to the volume fractions of methanol, water and associated methanol–water in the mobile phase, was fit to data in order to obtain solvation equilibrium constants for the interactions between the solute and water, the solute and methanol, and the solute and associated methanol–water. (The equilibrium constants are adjustable parameters in the model). They concluded that all three interactions are important, but interaction between the solutes they studied and free methanol contributes more to the retention process than interaction with associated methanol–water.

Both studies represent interesting approaches to solve a seemingly intractable problem, but the results of these studies are essentially parameter estimates obtained by fitting data to an assumed model; they must be used cautiously until their physical significance can be verified by some other means. It should also be noted that data for changes in the volume upon mixing relatively non-polar solutes with water, which Scott and coworkers used to support their model, has been interpreted in terms of packing of the solutes into the open structure of water, rather than association of the solute with water [37]. The complexity of these models will not be used in our solvation scheme.

Continuing with the derivation, it is postulated that the solvation free energy per molecule, ΔG^*_{solv}, is a weighted average of the solvation energy contributions $\Delta G^*_{RM_2}$, ΔG^*_{RMW}, and $\Delta G^*_{RW_2}$ from the three states RM_2, RMW, and RW_2, respectively. Mathematically, ΔG^*_{solv} is expressed by Eq. (6):

$$\Delta G^*_{solv} = \Delta G^*_{RM_2} F_{RM_2} + \Delta G^*_{RMW} F_{RMW} + \Delta G^*_{RW_2} F_{RW_2} \quad (6)$$

where, F_{RM_2}, F_{RWM}, and F_{RW_2} and are the fractions of the fully solvated, partially solvated and fully hydrated species in solution. Again, we use the superscript asterisk to indicate that these are apparent free energies of solvation which are calculated from concentrations rather than activities.

The sum of the three fractions in Eq. (6) is equal to 1, and it may be rearranged to give:

$$\Delta G^*_{solv} = \Delta G^*_{RM_2} + (S_1)F_{RMW} + (S_2)F_{RW_2} \quad (7)$$

Expressions for S_1 and S_2, given by Eqs. (8) and (9) respectively, are obtained from the thermodynamic cycles shown in Figs. 2 and 3.

$$S_1 = \Delta G^*_{RWM} - \Delta G^*_{RM_2} = -k_B T \ln \underline{K_1} \quad (8)$$

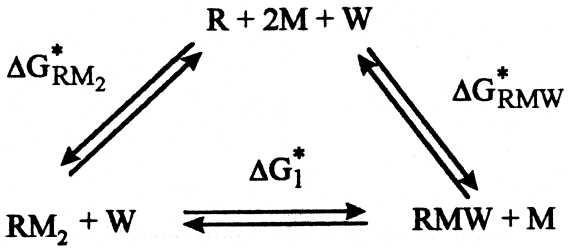

Fig. 2. The thermodynamic cycle used to obtain Eq. (8).

$$S_2 = \Delta G^*_{RW_2} - \Delta G^*_{RM_2} = -k_B T \ln \underline{K_1 K_2} \quad (9)$$

An explicit expressions for F_{RW_2} and F_{RWM}, given by Eqs. (10) and (11), are obtained by relating the solvation constants defined in Scheme 2 to the bulk mole fractions of water and organic cosolvent, x_1 and x_2, respectively.

$$F_{RW_2} = \frac{x_1^2 \underline{K_1 K_2}}{x_2^2 + x_1 x_2 \underline{K_1} + x_1^2 \underline{K_1 K_2}} \quad (10)$$

$$F_{RMW} = \frac{x_1 x_2 \underline{K_1}}{x_2^2 + x_1 x_2 \underline{K_1} + x_1^2 \underline{K_1 K_2}} \quad (11)$$

The final expression for the Solvation Effect is obtained by substitution of Eqs. (8)–(11) into Eq. (7) to give Eq. (12).

$$\Delta G^*_{solv} = \Delta G^*_{RM} + \left\{ \frac{(-k_B T \ln \underline{K_1}) \underline{K_1} x_1 x_2 - k_B T (\ln \underline{K_1 K_2}) \underline{K_1 K_2} x_1^2}{x_2^2 + x_1 x_2 \underline{K_1} + x_1^2 \underline{K_1 K_2}} \right\} \quad (12)$$

It should be noted that the exchange constants in Eqs. (10)–(12) are treated as composition independent terms. Such treatment requires that the product of the true thermodynamic constant and the appropriate activity coefficients be a constant or vary only slightly. This is a risky assumption; nevertheless, as we will see empirically in forthcoming sections, the solvation constants do possess constant values for a given solute in a given aqueous–organic mobile phase system. Moreover, we will see that they behave in a physically reasonable manner. It should be noted that composition dependent expressions for the Solvation Exchange Scheme could be developed, though at the expense of greater complexity. A basis for such an approach has been discussed by Eckert and co-workers [38], and may be tried at a later date.

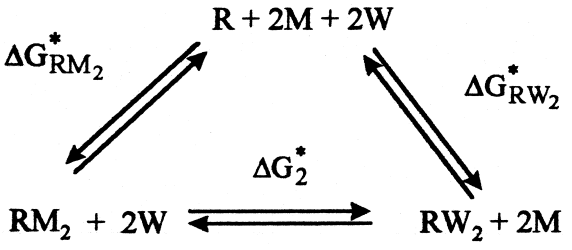

Fig. 3. The thermodynamic cycle used to obtain Eq. (9).

1.1.3. General medium effect

The General Medium Effect describes the energetic cost of creating, in the bulk solvent, a cavity to receive a solute. It is given by:

$$\Delta G^*_{gen.\ med.} = gA\gamma \quad (13)$$

where g is an empirical factor correcting for the surface curvature effect on surface tension, A is the surface area of the cavity which receives the solute, and γ is the surface tension. Horváth [15,16] derived a similar, though more sophisticated expression to account for solvent–solvent interactions. The curvature correction term in this expression is not an empirical factor as in Eq. (13), but a function of the molar volumes of the solvent and the solute species. It can be calculated a priori with values for the correction term in the pure solvent and the molar volumes of the solvent and solute species. In addition, the expression also considered the entropic cost of creating the cavity.

The surface tension in Eq. (13) is that of the solvation shell, and so it should reflect the solvent composition of the solvation shell, which may be different from that of the bulk.

To properly describe the surface tension of the solvation shell, gamma is defined by Eq. (14):

$$\gamma = \gamma_1 f_1 + \gamma_2 f_2 = \gamma_2 + (\gamma_1 - \gamma_2) f_1 \quad (14)$$

where γ_1 and γ_2 are the bulk surface tensions of water and organic cosolvent, respectively, and f_1 and f_2 are the mean fractional compositions of the solvation shell with respect to water and organic

solvent, respectively. An expression for f_1 is derived using the summation given by Eq. (15):

$$f_1 = \frac{1}{k} \sum i F_{\mathrm{RW}_i\mathrm{M}_j} \tag{15}$$

Here, the solvation stoichiometry is denoted by $\mathrm{RW}_i\mathrm{M}_j$ and $k = i + j$. For a two-step solvation scheme we write:

$$f_1 = \frac{F_{\mathrm{RMW}} + 2F_{\mathrm{RW}_2}}{2} \tag{16}$$

Combination of Eqs. (10), (11), (14), (16) with Eq. (13) gives the expression for the General Medium Effect:

$$\Delta G^*_{\mathrm{gen.med.}} = gA\gamma_2 + gA\gamma'' \frac{\underline{K_1}x_1x_2 + 2\underline{K_1K_2}x_1^2}{x_2^2 + x_1x_2\underline{K_1} + x_1^2\underline{K_1K_2}} \tag{17}$$

where $\gamma'' = \dfrac{\gamma_1 - \gamma_2}{2}$. Now to apply the model to retention data, we use the thermodynamic cycle in Fig. 4. (A similar approach was used to modify the model to describe complexation [27] and kinetic data [29]). In Fig. 4, *R* represents the solute in the mobile and stationary phases (denoted by superscripts m and s, respectively) as a gas or a liquid (denoted by subscripts g or l, respectively).

From Fig. 4 Eq. (18) is written where the free energy for partitioning of the solute (as a liquid) into the stationary phase (after vacating the mobile phase) is given by $\Delta G^*_{\mathrm{part,l}}$. The free energy for the analogous gas phase process is given by $\Delta G^*_{\mathrm{part,g}}$. The sum $\Delta G^*_{\mathrm{gen.\ med.}} + \Delta G^*_{\mathrm{solv}}$ corresponds to the transfer of the solute from the gas phase into solution in the liquid phase. According to Eq. (18), the partitioning of a solute between the mobile and stationary phases is controlled by the differences in the energy expended to create a solute-sized cavity in the mobile and stationary phases, and the differences in solvation energies attained by the solute in the mobile and stationary phases. The partition model states that retention is controlled by the differences of these energies also, but it uses binary interaction constants to describe these energies [17,18].

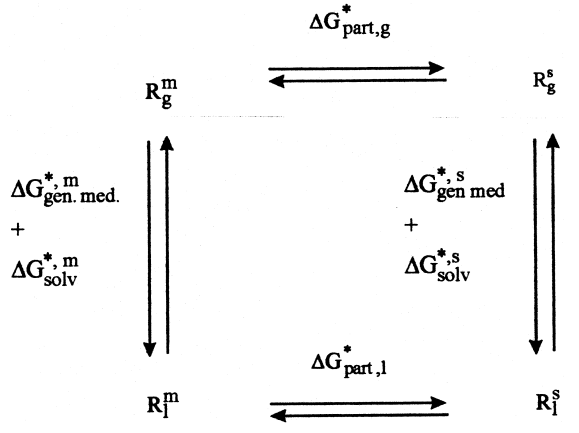

Fig. 4. Thermodynamic cycle for the partitioning of a solute into a stationary phase after vacating the mobile phase. The lower-half of the cycle represents the liquid phase, and the top-half represents the gas-phase.

$$\Delta G^*_{\mathrm{part,l}} = -(\Delta G^{*,\mathrm{m}}_{\mathrm{gen.\ med.}} + \Delta G^{*,\mathrm{m}}_{\mathrm{solv}}) + (\Delta G^{*,s}_{\mathrm{gen.\ med.}} + \Delta G^{*,s}_{\mathrm{solv}}) + \Delta G^*_{\mathrm{part,g}} \tag{18}$$

Eqs. (12) and (17) are substituted into Eq. (18) to give the explicit expression for $\Delta G^*_{\mathrm{part,l}}$; the expression is not shown here, but in the special case where $x_1 = 0$, a fully organic mobile phase, we get Eq. (19):

$$\Delta G^*_{\mathrm{part,l}} = \Delta G^{*,s}_{\mathrm{gen.med.}} + \Delta G^{*,s}_{\mathrm{solv}} + \Delta G^*_{\mathrm{part,g}} - gA^{\mathrm{m}}\gamma_2 - \Delta G^{*,\mathrm{m}}_{\mathrm{RM}_2} \tag{19}$$

where only the composition-independent terms remain.

Eq. (19) is written with the assumption that $\Delta G^{*,s}_{\mathrm{gen.med.}}$ and $\Delta G^{*,s}_{\mathrm{solv}}$ (the General Medium and Solvation Effects in the stationary phase) do not change with alterations in mobile phase composition. This is an extremely important assumption, and its validity will be discussed in the next section. At this point, for clarity, we will continue with the derivation.

The solvent effect on retention is related to the fully organic system using Eq. (20):

$$\delta_{\mathrm{m}}\Delta G^*_{\mathrm{part,l}} = \Delta G^*_{\mathrm{part,l}}(x_1) - \Delta G^*_{\mathrm{part,l}}(x_1 = 0) \tag{20}$$

where δ_{m} signifies a change in $\Delta G^*_{\mathrm{part,l}}$ induced by a medium effect.This operation eliminates the composition-independent terms and when applied to Eq. (18) gives:

$$\delta_m\Delta G^{*}_{part,l} = -\left(\delta_m\Delta G^{*,m}_{gen.med} + \delta_m\Delta G^{*,m}_{solv}\right) \quad (21)$$

Substitution of Eqs. (12) and (17) into Eq. (21) gives Eq. (22), the final equation for the Phenomenological Model.

$$\delta_m\Delta G^{*}_{part,l} = -\left\{\frac{\left(gA^m\gamma'' - k_BT\ln\underline{K_1^m}\right)\underline{K_1^m}x_1x_2 + \left(2gA^m\gamma'' - k_BT\ln\underline{K_1^mK_2^m}\right)\underline{K_1^mK_2^m}x_1^2}{x_2^2 + \underline{K_1^m}x_1x_2 + \underline{K_1^mK_2^m}x_1^2}\right\} \quad (22)$$

Eq. (22) is called a 'two-step model' as it was derived using a two-step solvation exchange scheme. The two-step model has three adjustable parameters, namely gA^m, $\underline{K_1^m}$ and $\underline{K_2^m}$.

A 'one-step model', given by Eq. (23), is similarly derived with a one-step solvation exchange scheme shown in Scheme 3.

All terms in Eq. (23) have been previously defined. The two adjustable parameters in Eq. (23) are gA^m, and $\underline{K_1^m}$.

$$\delta_m\Delta G^{*}_{part,l} = -\left\{\frac{\left(gA^m\gamma' - k_BT\ln\underline{K_1^m}\right)\underline{K_1^m}x_1}{x_2 + \underline{K_1^m}x_1}\right\} \quad (23)$$

Here, $\gamma' = \gamma_1 - \gamma_2$. Estimates of the parameters in both equations are obtained for each solute by non-linear regression of with x_1 and x_2 using Scientist® version 2.01., a non-linear regression, data fitting program. Both models will be used in this paper.

1.2. An important assumption

As was discussed, Eq. (19) was written with the assumption that solvent–solvent interactions in the stationary phase (described by $\Delta G^{*,s}_{gen.med}$) and solvent–solute interactions in the stationary phase (described by $\Delta G^{*,s}_{solv}$) are constant over all changes in mobile phase composition. We use this assumption in Eq. (19) to eliminate $\Delta G^{*,s}_{gen.med}$ and $\Delta G^{*,s}_{solv}$ from Eq. (22) which will be fit to the data. We are not saying that these terms do not exist or are unimportant, but only that they are constant for any mobile phase composition. Our data analysis and interpretation depend greatly on the validity of this assumption, and so a brief discussion of its soundness is necessary. The assumption is appropriate under three conditions. The first is that the solute fully embeds (or fully partitions) itself in the bonded octadecyl chains of the stationary phase rather than just adsorbs on the surface of the chains; the second condition is that components of the mobile phase (organic solvent and water) which are absorbed into the stationary phase does not interact strongly with the solute in the stationary phase. The third condition is that interactions between the solute and uncapped silanol groups of the stationary phase are minimal.

$$\mathbf{RM + W} \xrightleftharpoons{\underline{K_1}} \mathbf{RW + M}$$

Scheme 3.

There is much experimental evidence to support the existence of our first condition in RP-HPLC, namely that the solute does partition into the hydrocarbon chains of the stationary phase. For example, the work of Sentell and Dorsey [20] discussed earlier demonstrates that retention decreases at a critically high chain densities. This observation is not consistent with an adsorption mechanism, for increases in chain density would not be expected to decrease retention of a solute if it was only held on the surface of the bonded phase.

Works by Berendsen and De Galan [39] and Tchapla and co-workers [40,41] also suggest a partition mechanism is responsible for solute retention in RP-HPLC. These workers studied retention of variously sized solute molecules as a function of the bonded phase chain length. Retention was observed to increase with increases in chain length until the length approximated the linear dimensions of the investigated solute; at this critical chain length, retention no longer increased with increases in chain length. These observations are easily interpreted if a partition mechanism is assumed. Initially, the solute cannot fully embed itself in the shorter chains and is exposed to the mobile phase which causes it to elute off the column much faster than when the chains are longer. As the chain length is increased, the solute becomes increasingly embedded in the bonded phase, less exposed to the mobile phase and retention increases. At sufficient alkyl chain lengths, the solute becomes completely embedded in the stationary phase, and once the solute is fully surrounded by hydrocarbon, increases in chain

length do not change its hydrocarbon-like environment in the stationary phase, and retention does not increase. Berendsen and De Galan [39] also observed that the 'break point' in retention occurred at smaller chain lengths for solutes with polar functionalities. For example, the critical chain length for phenol was 7.3 methylene units while it was 9.6 units for benzene. They concluded that polar moieties, like a hydroxyl group, do not enter the stationary phase but remain outside it, immersed in the mobile phase. Tchapla and Heron [41] reached a similar conclusion from their data. Therefore, for molecules with polar functionalities, an adsorption/partition mechanism is probably at work, and in these cases, our assumption would be violated.

Recent work by Carr and co-workers [42–44] also suggests that retention of non-polar solutes with monomeric octadecane bonded phases [42] and polymeric octadecane bonded phases [44] occurs through a partition mechanism. (These workers examined phases of various lengths, from methane to octadecane, but we will restrict our discussion to octadecyl monomeric bonded phases which are pertinent to our studies). In these works, the transfer free energies of a methylene group from various methanol–water mixtures (mobile phase) to bulk liquid hexadecane were compared to the transfer free energies of a methylene group from methanol–water mixtures to bonded stationary phase. Clearly, the solute fully partitions into bulk liquid hexadecane, and if it fully partitions into the stationary phase, the transfer energies of both processes should be similar, with a ratio of about one. When mobile phases ranging from 0% to 70% methanol in water were used, the ratio of the transfer energy into bulk hexadecane to the transfer energy into octadecyl monomeric bonded phase was 1.1 to 1.4 depending on the column brand. When mobile phases consisting of greater than 70% methanol in water were used, the ratios were larger and at 100% methanol approached or exceeded a value of 2. Similar work with polar solutes [43] demonstrated that the ratio of the transfer energy into bulk hexadecane and the transfer energy into octadecyl stationary phases were quite different over most mobile phase compositions.

The explanation for the observed behavior of non-polar methylene groups in mobile phases with less than 70% methanol is simple; retention is occurring through a partition-like process, and therefore our assumption is valid under these conditions. The explanation for the observed behavior of methylene groups in organic-rich mobile phases and of polar solutes is more complicated, as two events could lead to such behavior. The first is that the solute does not partition fully into the stationary phase, but only adsorbs mostly on the surface; retention occurs via an adsorption mechanism. The second is that the solute partitions fully into the stationary phase, but it interacts very strongly with mobile phase components absorbed into the stationary phase so that the stationary phase is not accurately represented by a bulk hydrocarbon. (In these works, Carr and co-workers acknowledge that determination of capacity factors in organic-rich mobile phases becomes difficult owing to the low retention of the solutes and that their results should not be considered as final. However, despite the possible error in the experimental measurements, their explanation does seem reasonable, and the data follow a clear and convincing trend where the energy ratio approaches or exceeds a value of 2). Earlier work by Carr [12] suggests that non-polar solutes do not interact strongly with methanol and water (relative to their interaction with hydrocarbon chains), and therefore, the first event is the likely cause for the observed behavior. His work with polar solutes, which could interact strongly with mobile phase components via dipole–dipole interactions (hydrogen-bonding interactions) suggests that both events could be occurring [43]. For our purposes, defining which event occurs is not as important as realizing that both could jeopardize the soundness of our assumption, and our data must be carefully inspected, particularly data for polar and semi-polar solutes.

Thus far, we have presented evidence to support that retention occurs via a partition mechanism (especially retention of non-polar molecules). Similar to solutes, it should be expected that components of the mobile phase (organic solvent and water) will also enter the stationary phase, and indeed a large quantity of experimental evidence exists to support this idea [45–54]. The amounts of organic solvent and water that enter the stationary phase depend on the organic solvent used (the order of absorption into the stationary phase is methanol$<$acetonitrile$<$ tetrahydrofuran) and its concentration within the

mobile phase [45–48,51,52]. These components could interact with embedded solutes, and the strength of these interactions would vary with the amounts of organic solvent and water absorbed into the stationary phase and therefore depend on the mobile phase composition. This situation is a violation of our assumption that solvent–solute interaction energies within the stationary phase are independent of mobile phase composition. However, if the interactions between the embedded solute and mobile phase components are insignificant relative to interactions between the solute and the bonded phase, then, to a first approximation, our assumption is valid.

Carr and co-workers [12] have addressed this point by comparing transfer free energies of non-polar methylene groups from gas phase to hexadecane and from gas phase to various methanol–water mixtures. In all cases, the transfer free energies from gas phase to hexadecane were much larger (about 600 cal/mole greater in some cases) than the transfer free energies from gas phase to the methanol–water mixtures. The study suggests that interactions between non-polar solutes and alkyl chains of the stationary phase are much greater than those between non-polar solutes and relatively polar mobile phase components. However, in later work [43], the transfer free energies of various polar moieties (OCH_3, $COOCH_3$, CHO, CN, NO_3) from gas phase to hexadecane and from gas phase to methanol–water mixtures (mobile phase) were compared. In these studies, the energies for transfer into mobile phase were always much greater (about 270 cal/mole to 1600 cal/mole greater depending on the moiety) than the energies for transfer into hexadecane. Clearly, interactions between the polar solutes and absorbed mobile phase components (which are probably attributable to hydrogen bonding) cannot be ignored. McCormick and Karger [46] have even suggested such interactions can be exploited to control selectivity of polar solutes by using ternary mobile phases consisting of non-typical organic solvents such as trifluoroethanol and hexafluoroisopropanol. Carr's studies indicate that our assumption is probably not justified for polar and semi-polar solutes which interact strongly with mobile phase components present in the stationary phase, and the results of our work, particularly for polar solutes, must be carefully examined. By analogy, interactions between polar solutes and uncapped silanol groups within the stationary phase would also invalidate our assumption.

2. Experimental

2.1. Retention studies

2.1.1. Materials

The organic solvents, methanol (MeOH) and chloroform, used in our studies were of HPLC grade and were obtained from EM Science (Gibbstown, NJ, USA). Distilled, deionized water was obtained from an in-house Barnstead/Thermolyne PCS water purification system that consisted of pre-filter, organic, ion-exchange, and microfilter (0.2-μm) cartridges (Barnstead, Dubuque, IA, USA).

The four solutes used in our studies, benzene, naphthalene, bromobenzene and 1-iodonaphthalene, were obtained from Aldrich Chemical Company (Milwaukee, WI, USA); all were greater than 98% purity and were used as received.

2.1.2. Apparatus

A Perkin-Elmer Lambda 4B UV/VIS Spectrophotometer with 1-cm quartz cuvettes (Sigma Chemical, St. Louis, MO, USA) was used to obtain UV spectra of all solutes used in these studies.

Retention times for all studies were determined with the following chromatographic system. A Knauer HPLC Pump Model 64 (Sonnteck, Woodcliff Lake, NJ, USA), was used for solvent delivery, and a Knauer Variable Wavelength UV/VIS Monitor (Sonnteck), was used for detection. Samples were injected onto an Alltima, 5-μm, 150×4.6 mm base-deactivated octadecyl RP-HPLC column (Alltech Associates, Deerfield, IL, USA), using a Rheodyne Model 7125 manual injector (Cotati, CA, USA) fitted with a 20-μl sample loop. A Hamilton (Reno, NV, USA) 725 SNR LC syringe was used to manually fill the loop. Data acquisition and analysis were performed with a Hitachi D-2500 Chromato-Integrator (Mt. View, CA, USA). The temperatures of the column and mobile phase were maintained at 35.0±0.1°C in a large water bath with an Allied

Fisher Scientific Thermoregulator Model 70 (Pittsburgh, PA, USA).

2.2. Procedures

2.2.1. Binary aqueous organic cosolvent preparation

Typically, 10 to 13 binary methanol–water cosolvent solutions were prepared for each solute studied; the solvent compositions of the solutions were varied from pure methanol to pure water until elution of the solutes was no longer observed. These solutions were prepared by measuring separately and then mixing known weights of methanol and water. All mixtures were filtered and degassed under vacuum before they were used. The weight of each component was recorded and used later to calculate the mole fractions of methanol and water in the mobile phase.

2.2.2. Sample preparation

Solutes were dissolved in methanol and diluted to appropriate concentrations for chromatographic and spectrophotometric analyses. The concentrations used for chromatographic analyses were: benzene 1.46×10^{-3} *M*, naphthalene 1.56×10^{-4} *M*, bromobenzene 7.49×10^{-4} *M* and 1-iodonaphthalene 3.99×10^{-4} *M*.

2.2.3. Analytical methods

UV absorption spectra of benzene, naphthalene, bromobenzene and 1-iodonaphthalene were recorded to obtain the wavelengths of maximum absorbance that were used for detection of the solutes during chromatographic studies. These wavelengths were: benzene at 254 nm, naphthalene at 275 nm, bromobenzene at 287 nm and 1-iodonaphthalene at 260 nm. All spectra possessed broad bands at these wavelengths.

All chromatographic analyses were performed at a flow-rate of 1.0 ml/min, and the column was equilibrated for at least 1 h before making any injections. Retention time determinations were carried out at least in duplicate for each solute in each methanol–water system.

2.2.4. Determination of void volume

The void volume was determined with a gravimetric technique similar to that used by McCormick and Karger [45] and Sentell and Dorsey [20]. Over 100 ml of methanol was flowed through the column which was removed, sealed and weighed on an analytical balance. The process was repeated with chloroform. Densities for chloroform and methanol were determined at 35.0 ± 0.1°C (the temperature at which the column was equilibrated) using a thermostated pycnometer. The void volume was calculated by dividing the difference in the weight of the column when filled with chloroform and methanol by the difference in the densities of the two liquids. It is 1.58 ± 0.044 ml.

2.2.5. Determination of void time

To accurately determine the void time, t_m, the column void volume was corrected for extra-column volume using the known dimensions of the column tubing and the detector flow cell. The corrected void volume was then divided by the exact flow-rate of the pump determined as follows.

Water was flowed through the entire system for 1 h and then collected at the detector outlet for 20 to 25 min in a tarred graduated cylinder. The weight of water collected was converted to volume using the density, and the volume was divided by the time of collection. The average flow-rate (of four determinations) was 0.965 ± 0.0077 ml/min. The void time, t_m, is 1.680 ± 0.047 min.

2.2.6. Surface area determination

The actual molecular surface area of the solutes was determined using a simple, inexpensive, non-calculational method described by Khossravi and Connors [21]. A molecular model of each non-polar solute was constructed using a Corey–Pauling–Koltun (CPK) space-filling model kit (Ealing, South Natick, MA, USA). The models were wrapped tightly with aluminum foil, ignoring fine features so that the wrapped model resembled a smooth shell. The aluminum foil is intended to represent the solvent accessible surface area of the molecule. After wrapping, the aluminum foil was removed and weighed; this weight was converted to an area through a standard curve relating surface areas (based on linear dimensions) of aluminum foil squares to their respective weights.

For reasons explained later, we were interested in

determining the non-polar surface area of the molecules studied. Most of the molecules examined in this work are completely non-polar, and thus the non-polar surface area was determined by wrapping the entire molecule ($A_{nonpolar} = A_{total}$). In the case of phenol, a semi-polar solute, a subjective judgment of non-polar surface area (essentially the aromatic phenyl ring minus the edge effect from the hydroxyl group) was required and only this portion of the molecule was wrapped.

2.3. Calculations

The solvent effect on the apparent free energy for the partitioning of the solute from the mobile phase into the stationary phase is accurately calculated from experimental data using Eq. (24).

$$\delta_m \Delta G^*_{part,l} = -k_B T \ln\left(\frac{k'}{k'_{org}}\right) + k_B T \ln\left(\frac{\varphi}{\varphi_{org}}\right) \quad (24)$$

where k' is the capacity factor of the solute at any mobile phase composition, φ is the phase ratio at any mobile phase composition, and the subscript, org, indicates the value in a fully organic mobile phase ($x_2 = 1$). All other terms have been previously defined.

The phase ratio is the ratio of the stationary phase volume, V_s, to the mobile phase volume, V_m, and is calculated from these quantities. The gravimetric technique [20,45] discussed earlier can be used to estimate V_m, and Sentell and Dorsey [20] have used an equation to calculate V_s. The values for V_m and V_s so obtained would be constant for a given column, and thus give a value for φ that would be constant for a column and would not vary with mobile phase composition. Some workers have treated φ as a constant for the column [55]. In this case, $\varphi = \varphi_{org}$ and Eq. (24) reduces to:

$$\delta_m \Delta G^*_{part,l} = -k_B T \ln\left(\frac{k'}{k'_{org}}\right) \quad (25)$$

Given the earlier discussion concerning partition of mobile phase components into the stationary phase, it cannot be assumed that V_m is constant over all mobile phase compositions. In addition, V_s would change with alterations in the configuration of the octadecyl chains of the stationary phase, which assume a folded configuration in water-rich mobile phases and an extended configuration in organic-rich mobile phases [42,47]. The situation is complicated further if one considers that the absorbed mobile phase components are part of the stationary phase. (The question becomes where does the mobile phase begin and the stationary phase end?) However, Eq. (25) can be used as an approximation if $|\ln(k'/k'_{org})| > |\ln(\varphi/\varphi_{org})|$. It is difficult to assess the correctness of this approximation as determination of the phase ratio is difficult – different experimental techniques lead to different estimates of [52,56]. For example, values for V_m determined (via D_2O injections) by Karger and McCormick [45] for a C_8 column as a function of mobile phase composition in methanol–water mixtures vary only from 1.19 ml to about 1.16 ml with the minimum value at about 60% methanol in water. (If V_s varies by the same extent, then the phase ratio would change very little over the mobile phase composition, and the aforementioned approximation is appropriate.) However, values for a C_8 column in methanol–water mobile phases determined by Yonkers and co-workers [47] using a different technique vary from 1.29 ml to 0.755 ml with the minimum at 100% methanol. Given such uncertainty in estimating values for and the even greater uncertainty of determining values for, we will use Eq. (25) as an approximation.

2.4. Treatment of literature data

Retention data for non-polar solutes, similar to the solutes used in our study, reported by Schoenmakers and co-workers [57] were analyzed to further test the model. We also tested data for phenol, a representative semi-polar solute. These workers studied retention of these solutes with MeOH–water, MeCN–water and THF–water mobile phases in which the concentration of organic solvent was varied from 100% to 10%. They found that Eq. (2) could accurately describe the data up to $k' = 50$ and reported the coefficients *A*, *B*, and *C* obtained by fitting the equation to the data. Using these coefficients, values for $\ln k'$ were calculated (only for k' as high as 50, so *no extrapolation* was involved) as a function of volume fraction organic ('the experimental data points'). To apply the data to the

model, the volume fractions of the organic solvents were converted to mole fractions by interpolation of data given in Refs. [29,58].

3. Results and discussion – part one

3.1. Two-step model – Eq. (22)

3.1.1. Curve fits

The chromatographic data from our studies are reported in Tables 1–4, and the parameter estimates, obtained by fitting Eq. (22) to our data and to data from Schoenmakers and co-workers [57] are presented in Tables 5 and 6, respectively. The fits to the data can be assessed from the coefficient of determination (r^2) value and the curve fit criterion given in Tables 5 and 6. (Curve fit criterion = 100% × standard deviation of the points about the fitted line/absolute value of the mean of ordinate values; a smaller number indicates a better fit). The average values ± one standard deviation of the curve fit criteria in Tables 5 and 6 are: 0.5±0.38 (n=10) for methanol–water mobile phases, 0.4±0.29 (n=7) for acetonitrile–water mobile phases (the data for phenol were not included in this average for reasons subsequently described), and 1.6±0.24 (n=8) for tetrahydrofuran–water mobile phases. These values indicate that the fits to the data are better for methanol–water and acetonitrile–water systems than for tetrahydrofuran–water systems.

The poorer fits for the tetrahydrofuran–water mobile phases could be attributable to solvation of the solutes by absorbed mobile phase components. As previously discussed, experimental evidence [45–48] has shown that THF is absorbed into the stationary phase to a greater extent than methanol and acetonitrile; therefore, the potential for solvation of solutes within the stationary phase is greater for THF than the other solvents. Significant solvation of the solutes within the stationary phase violates a key assumption of the model, namely that interactions between absorbed mobile phase components and the absorbed solute are negligible. Alternatively, one could argue that solutes are retained by a partition mechanism when methanol or acetonitrile are used, and by an adsorption/partition mechanism when tetrahydrofuran is used. This situation would also violate the model's assumption.

Figs. 5–8 show representative plots of $\delta_m \Delta G^*_{part,l}$ against x_2 for several solutes with methanol–water, acetonitrile–water, and tetrahydrofuran–water mobile phases; the points are the experimental data points, and the smooth curve was obtained by fitting

Table 1
Solvent effect data for benzene retention in methanol–water binary cosolvent systems

Mole fraction Organic (x_2)	Capacity factor (k')[a]	$\delta_m \Delta G^*_{part,l}$ /10^{-20} J per molecule	$\delta_m \Delta G^*_{part,l}$ /10^{-20} J per molecule Calculated from fit of Eq. (22) to data	$\delta_m \Delta G^*_{part,l}$ /10^{-20} J per molecule Calculated from fit of Eq. (23) to data
0.1232	29.5 (0.37)[b]	−2.12 (0.013)[c]	−2.123	−2.127
0.1577	21.68 (0.022)	−1.99 (0.012)	−1.985	−1.986
0.1941	15.6 (0.24)	−1.85 (0.013)	−1.847	−1.846
0.2727	8.4 (0.15)	−1.58 (0.014)	−1.572	−1.568
0.3125	6.03 (0.020)	−1.44 (0.012)	−1.443	−1.440
0.3544	4.407 (0.0084)	−1.31 (0.012)	−1.315	−1.313
0.4576	2.2 (0.12)	−1.02 (0.026)	−1.028	−1.028
0.5660	1.222 (0.0042)	−0.77 (0.012)	−0.766	−0.768
0.6909	0.674 (0)	−0.51 (0.012)	−0.504	−0.509
0.8311	0.368 (0.0024)	−0.25 (0.012)	−0.253	−0.257
1.0000	0.202 (0.0056)	0.00 (0.017)	0	0

Chromatographic conditions: Flow-rate = 1.0 ml/min, C_{18} base-deactivated column, temperature of mobile phase and column 35.0±0.1°C.
[a] $\left(k' = \frac{t_r - t_m}{t_m}\right)$; t_m = 1.68±0.047 min.
[b] Numbers in parentheses are standard deviations (S.D.).
[c] Calculated by standard propagation of errors.

Table 2
Solvent effect data for naphthalene retention in methanol–water binary cosolvent systems

Mole fraction Organic (x_2)	Capacity factor (k')[a]	$\delta_m\Delta G^*_{part,l}$ /10^{-20} J per molecule	$\delta_m\Delta G^*_{part,l}$ /10^{-20} J per molecule Calculated from fit of Eq. (22) to data	$\delta_m\Delta G^*_{part,l}$ /10^{-20} J per molecule Calculated from fit of Eq. (23) to data
0.2728	40.623 (0)[b]	−1.999 (0.0028)[c]	−2.001	−1.995
0.2732	40.464 (0)	−1.998 (0.0028)	−1.999	−1.993
0.3364	20.12 (0.03)	−1.701 (0.0028)	−1.697	−1.702
0.3594	15.948 (0)	−1.602 (0.0028)	−1.599	−1.605
0.3601	15.766 (0.022)	−1.597 (0.0028)	−1.596	−1.602
0.4576	6.58 (0.12)	−1.225 (0.0082)	−1.233	−1.236
0.5673	3.003 (0.0072)	−0.892 (0.0030)	−0.899	−0.896
0.6913	1.514 (0.056)	−0.601 (0.016)	−0.587	−0.579
0.8339	0.717 (0.012)	−0.284 (0.0076)	−0.289	−0.282
1.0000	0.368 (0.0024)	0.00 (0.0039)	0	0

Chromatographic conditions are as specified in Table 1.
[a] $\left(k' = \frac{t_r - t_m}{t_m}\right)$; $t_m = 1.68 \pm 0.047$ min.
[b] Numbers in parentheses are standard deviations (S.D.).
[c] Calculated by standard propagation of errors.

Eq. (22) to the data. Points for all the solutes studied with MeOH–water and THF–water mobile phases and the non-polar solutes studied with MeCN–water mobile phases follow a hyperbolic pattern. The hyperbolic pattern of these points indicates that the solute is least retained when a fully organic mobile phase is used, and retention increases as water is added. (Such a trend is expected for retention of these non-polar solutes and phenol on a C_{18} column). Visual inspection of the plots, and the values for r^2 and curve fit criterion demonstrate that the fits to the data are good for these systems.

Table 3
Solvent effect data for bromobenzene retention in methanol–water binary cosolvent systems

Mole fraction Organic (x_2)	Capacity factor (k')[a]	$\delta_m\Delta G^*_{part,l}$ /10^{-20} J per molecule	$\delta_m\Delta G^*_{part,l}$ /10^{-20} J per molecule Calculated from fit of Eq. (22) to data	$\delta_m\Delta G^*_{part,l}$ /10^{-20} J per molecule Calculated from fit of Eq. (23) to data
0.1943	64.686 (0)[b]	−2.290 (0.0024)[c]	−2.300	−2.282
0.2324	41.1 (0.15)	−2.097 (0.0029)	−2.087	−2.087
0.2726	26.27 (0.079)	−1.907 (0.0028)	−1.887	−1.898
0.3151	15.97 (0.031)	−1.695 (0.0026)	−1.700	−1.714
0.3597	10.28 (0.020)	−1.508 (0.0026)	−1.523	−1.536
0.4573	4.817 (0.0025)	−1.186 (0.0025)	−1.190	−1.194
0.5672	2.265 (0.0013)	−0.865 (0.0025)	−0.878	−0.871
0.6296	1.637 (0.0030)	−0.727 (0.0026)	−.723	−0.711
0.6909	1.233 (0.0010)	−0.606 (0.0025)	−.582	−0.568
0.8327	0.579 (0.0084)	−0.285 (0.0066)	−.293	−0.279
1.0000	0.296 (0.0017)	0.000 (0.0035)	0	−0

Chromatographic conditions are as specified in Table 1.
[a] $\left(k' = \frac{t_r - t_m}{t_m}\right)$; $t_m = 1.68 \pm 0.047$ min.
[b] Numbers in parentheses are standard deviations (S.D.).
[c] Calculated by standard propagation of errors.

Table 4
Solvent effect data for 1-iodonaphthalene retention in methanol–water binary cosolvent systems

Mole fraction organic (x_2)	Capacity factor (k')[a]	$\delta_m\Delta G^*_{part,l}$ /10^{-20} J per molecule	$\delta_m\Delta G^*_{part,l}$ /10^{-20} J per molecule Calculated from fit of Eq. (22) to data	$\delta_m\Delta G^*_{part,l}$ /10^{-20} J per molecule Calculated from fit of Eq. (23) to data
0.3600	57.3 (0.43)[b]	−1.856 (0.0061)[c]	−1.855	−1.853
0.3787	45.2 (0.27)	−1.756 (0.0058)	−1.758	−1.757
0.4073	33.4 (0.14)	−1.627 (0.0055)	−1.618	−1.619
0.4572	19.22 (0.017)	−1.392 (0.0052)	−1.398	−1.400
0.5108	11.60 (0.075)	−1.177 (0.0059)	−1.188	−1.190
0.5665	7.551 (0.011)	−0.995 (0.0052)	−0.996	−0.996
0.6271	5.023 (0.046)	−0.822 (0.0065)	−0.808	−0.808
0.6922	3.184 (0.016)	−0.627 (0.0056)	−0.630	−0.629
0.7600	2.191 (0.013)	−0.469 (0.0052)	−0.465	−0.462
0.8333	1.505 (0.0045)	−0.22 (0.0035)	−0.305	−0.303
0.9139	0.992 (0.0069)	−0.088 (0.0039)	−0.149	−0.147
1.0000	0.727 (0.0089)	0.000 (0.0047)	0.000	0.000

Chromatographic conditions are as specified in Table 1.
[a] $\left(k' = \frac{t_r - t_m}{t_m}\right)$; $t_m = 1.68 \pm 0.047$ min.
[b] Numbers in parentheses are standard deviations (S.D.).
[c] Calculated by standard propagation of errors.

The plot of $\delta_m\Delta G^*_{part,l}$ vs. x_2 for phenol with MeCN–water mobile phases is unexpectedly parabolic rather than hyperbolic. The parabolic shape of this plot indicates that phenol is least retained in a mixed aqueous–organic system rather than a fully organic system (see Fig. 7). The fits to these data are not as good as indicated by the large curve fit criterion (5.530) for this system and the plot of the residuals (residuals = observed values–estimated values) shown in Fig. 9; the residuals are much larger than the residuals for the two other solutes shown in the figure. Furthermore, the parameter estimates for phenol in the acetonitrile–water system do not possess physically realistic values. For example, the molecular surface area term is negative ($gA^m = -0.53$). The anomalous behavior could be due to solvation of phenol by absorbed acetonitrile and water in the stationary phase, or one could argue that phenol is retained by an adsorption/partition mechanism when acetonitrile is used. However, based on previous discussions, such behavior (poor fits and unrealistic parameter estimates) would be expected

Table 5
Parameter estimates, curve fitting data and estimates of molecular surface areas for benzene, bromobenzene, naphthalene and 1-iodonaphthalene retention data. Parameter estimates obtained by fitting Eq. (22) to the data

Solute	gA^m (S.D.)/Å^2 per molecule	Area (S.D.) /Å^2 per molecule	$\underline{K_1^m}$ (S.D.)	$\underline{K_2^m}$ (S.D.)	r^2 Curve fit[a]
Benzene	47.4 (0.35)	108 (1.5)	1.30 (0.033)	0.33 (0.012)	0.9999 0.628
Bromobenzene	69 (4.6)	144 (2.2)	0.96 (0.065)	0.15 (0.041)	0.9997 1.202
Naphthalene	76 (7.5)	147 (3.0)	0.82 (0.085)	0.14 (0.047)	0.9999 0.596
1-Iodonaphthalene	120 (680)	188 (4.4)	0.5 (2.9)	0.07 (1.2)	0.9998 0.956

[a] Curve fit criterion = 100% × standard deviation of the points about the fitted line/absolute value of the average of ordinate values.

Table 6
Parameter estimates obtained by fitting Eq. (22) to data from Schoenmakers and co-workers [57]

Solute	Solvent	gA^m (S.D.)/Å^2 per molecule	Area (S.D.) /Å^2 per molecule	$\underline{K_1^m}$ (S.D.)	$\underline{K_2^m}$ (S.D.)	r^2 Curve fit[a]
Benzene	Methanol	34.48 (0.08)	108 (1.5)	0.866 (0.0046)	0.272 (0.0027)	1.0000 0.187
Biphenyl	Methanol	75 (1.7)	179 (3.0)	0.66 (0.015)	0.18 (0.011)	1.0000 0.109
Chlorobenzene	Methanol	52.9 (0.46)	129 (2.5)	0.505 (0.0026)	0.219 (0.0053)	0.9998 0.159
Ethylbenzene	Methanol	58.9 (0.74)	153 (7.4)	0.643 (0.0064)	0.206 (0.0076)	1.0000 0.165
Phenol	Methanol	18.63 (0.096)	74 (3.1)	0.513 (0.0063)	0.206 (0.0026)	1.0000 0.426
Toluene	Methanol	49.5 (0.46)	129 (3.0)	0.56 (0.0033)	0.215 (0.0058)	1.0000 0.173
Benzene	Acetonitrile	23.4 (0.57)	108 (1.5)	0.345 (0.0084)	0.155 (0.0061)	0.9999 0.993
Biphenyl	Acetonitrile	42.0 (0.28)	179 (3.0)	0.359 (0.0013)	0.216 (0.0042)	1.0000 0.193
Chlorobenzene	Acetonitrile	29.0 (0.3)	129 (2.5)	0.286 (0.0033)	0.220 (0.007)	1.0000 0.469
Ethylbenzene	Acetonitrile	34.4 (0.19)	153 (7.4)	0.375 (0.0016)	0.207 (0.0035)	1.0000 0.200
Naphthalene	Acetonitrile	33.2 (0.15)	147 (3)	0.522 (0.0030)	0.197 (0.0032)	1.0000 0.236
Phenol	Acetonitrile	−0.53 (0.53)	74 (3.1)	0.08 (0.015)	0.27 (0.066)	0.9973 5.530
Toluene	Acetonitrile	30.0 (0.33)	129 (3.0)	0.322 (0.0046)	0.190 (0.0067)	1.0000 0.605
Anthracene	Acetonitrile	43.1 (0.57)	188 (4.3)	0.504 (0.0037)	0.195 (0.0076)	1.0000 0.287
Benzene	THF	20.3 (0.54)	108 (1.5)	0.150 (0.0050)	0.100 (0.0064)	0.9997 1.496
Biphenyl	THF	32 (1.1)	179 (3.0)	0.131 (0.0046)	0.16 (0.015)	0.9998 1.401
Chlorobenzene	THF	25 (1.1)	129 (2.5)	0.104 (0.0059)	0.17 (0.02)	0.9995 2.059
Ethylbenzene	THE	31.2 (0.93)	153 (7.4)	0.171 (0.0044)	0.115 (0.0089)	0.9998 1.258
Phenol	THF	8.8 (0.32)	74 (3.1)	0.143 (0.0053)	0.097 (0.0049)	0.9997 1.522
Naphthalene	THF	25 (1.2)	147 (3)	0.083 (0.0060)	0.25 (0.035)	0.9998 1.530
Toluene	THF	25 (1.0)	129 (3.0)	0.131 (0.0052)	0.14 (0.013)	0.9997 1.653
Anthracene	THF	34 (1.3)	188 (4.3)	0.110 (0.0051)	0.19 (0.021)	0.9997 1.657

[a] Curve fit criterion = 100% × standard deviation of the points about the fitted line/absolute value of the average of ordinate values.

to also occur with the tetrahydrofuran–water system. The fact that it does not suggests that the unusual behavior for phenol in the acetonitrile–water phases may be due to a problem in the original data. Perhaps the accuracy of the data was compromised during its fitting to Eq. (2) and so the data we

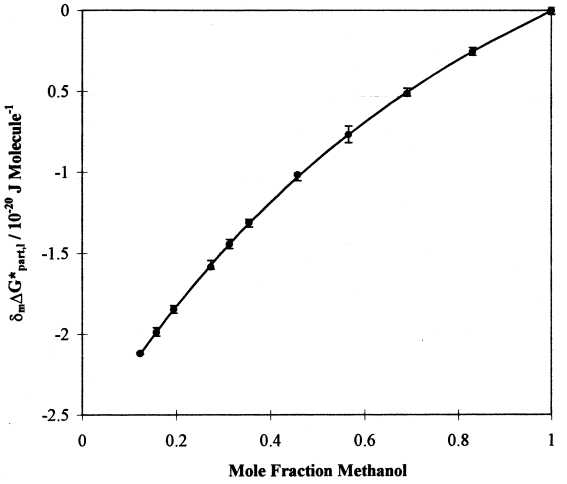

Fig. 5. Solvent effect on the retention of benzene in methanol–water binary cosolvent systems showing the experimental data points and the fitted curve for the two-step model [Eq. (22)]. The error bars are twice the standard deviation of $\delta_m\Delta G^*_{part,l}$. Chromatographic conditions: Flow-rate = 1.0 ml/min, C_{18} base-deactivated column, temperature of mobile phase and column = 35.0±0.1°C.

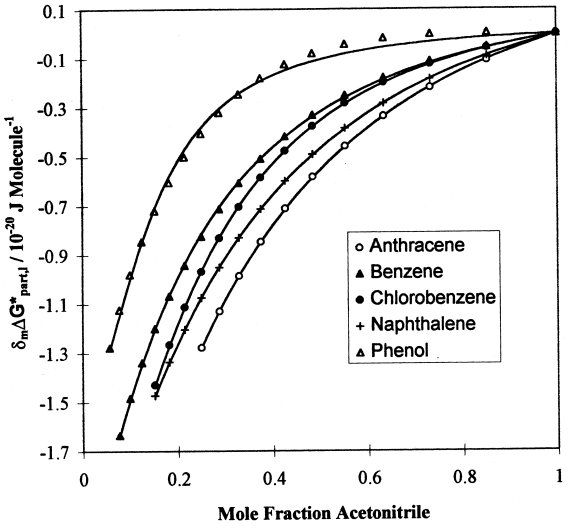

Fig. 7. Fits to data of various solutes in acetonitrile–water mobile phases. (Data from Schoenmakers and coworkers [57]). The points are experimental, and the smooth curve is the fit of Eq. (22) to the data. Chromatographic conditions: Silica-based C_{18} column (30×4.6 cm) Flow-rate = 1.5 ml/min, temperature = 25°C.

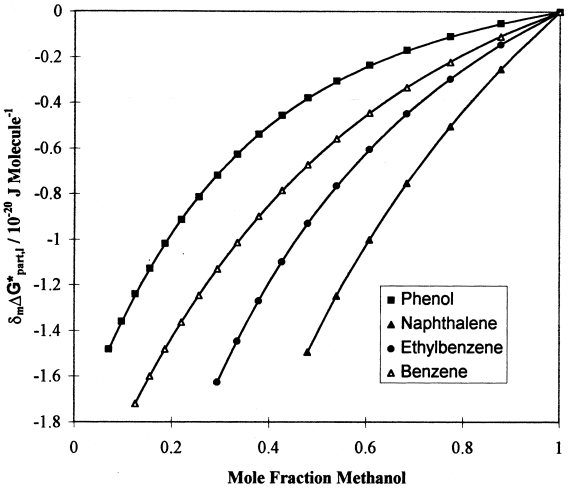

Fig. 6. Fits to data of various solutes in methanol–water binary cosolvent systems. (Data from Schoenmakers and coworkers [57]). The points are experimental, and the smooth curve is the fit of Eq. (22) to the data. Chromatographic conditions: Silica-based C_{18} column (30×4.6 cm) Flow-rate = 1.5 ml/min, temperature = 25°C.

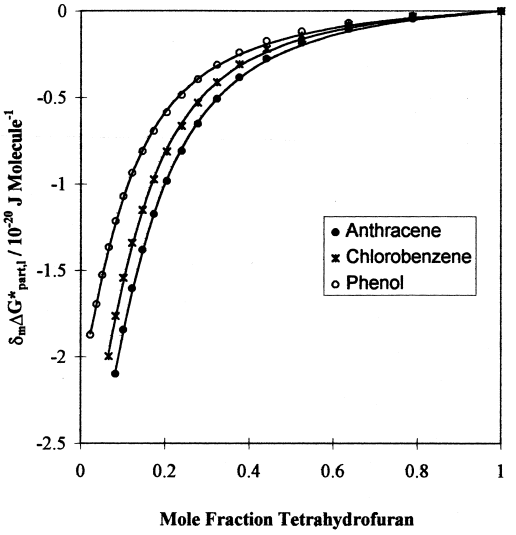

Fig. 8. Fits to data of various solutes in tetrahydrofuran–water mobile phases. (Data from Schoenmakers and coworkers [57]). The points are experimental, and the smooth curve is the fit of Eq. (22) to the data. Chromatographic conditions: Silica-based C_{18} column (30×4.6 cm) Flow-rate = 1.5 ml/min, temperature = 25°C.

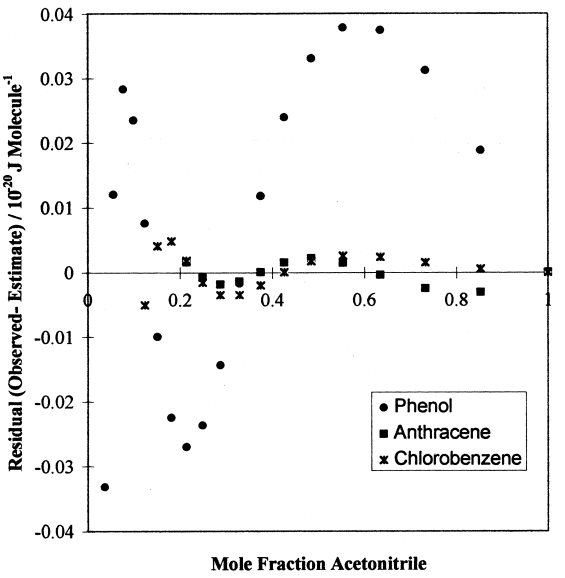

Fig. 9. The residuals of fits to the data for some solutes in Fig. 7.

generated and analyzed is not accurate. Owing to the potential inaccuracy of these data, they will not be analyzed further.

3.1.2. The parameter estimates

The two-step model (Eq. (22)), with a few exceptions, can quantitatively describe changes in retention as a function of mole fraction organic solvent in the mobile phase; however, if the model is physically correct, then the parameter estimates, obtained by fitting the model to these data, must possess some physical significance. In the next two sections, we will discuss the physical significance of the solvation exchange constants and the gA^m parameter estimates obtained by analysis of the literature data [57]. We defer discussion of our data to Section 4.

3.1.2.1. Solvation exchange constants

The average values (± 1 standard deviation) for the exchange constants in Table 6 are: $\underline{K_1^m} = 0.6 \pm 0.13$ and $\underline{K_2^m} = 0.22 \pm 0.030$ for methanol–water ($n = 6$); $\underline{K_1^m} = 0.39 \pm 0.090$ and $\underline{K_2^m} = 0.20 \pm 0.022$ for acetonitrile–water ($n = 7$, the questionable phenol data was excluded); and $\underline{K_1^m} = 0.13 \pm 0.028$ and $\underline{K_2^m} = 0.15 \pm 0.052$ for THF–water ($n = 8$). The solvation exchange constants appear to be relatively independent of the solute structure, but appear to decrease as the polarity of the organic solvent in the mobile phase decreases. This variation is consistent with the solvation scheme shown in Scheme 2 where the solvation constants indicate the degree to which organic solvent is displaced from the solvation shell by water. For non-polar and semi-polar solutes, $\underline{K_1^m}$ and $\underline{K_2^m}$ are expected to possess smaller values for solvents in which the solutes are more miscible (solvents of lower polarity) and higher values for solvents in which the solutes are less miscible (more polar solvents which are more easily displaced from the solvation shell by water). To explore this behavior, $\ln \underline{K_1^m}$ and $\ln \underline{K_1^m K_2^m}$ were plotted against Log P (the logarithm of the octanol–water partition coefficient) of the organic solvent in solution. (Log P is used as a measure of solvent polarity, smaller values indicate higher polarity.) The plot shown in Fig. 10 demonstrates that tetrahydrofuran, the least polar of the solvents, possesses the smallest $\ln \underline{K_1^m}$ and $\ln \underline{K_1^m K_2^m}$ values and methanol, the most polar of the solvents, possesses the largest values. Aside from demonstrating that the solvation exchange constants are varying in a physically reasonable manner, Fig. 10 also provides means to obtain rough estimates for the solvation exchange constants.

It should be noted that the relative standard deviations of most of the solvation exchange constants given in Table 6 are larger than the relative

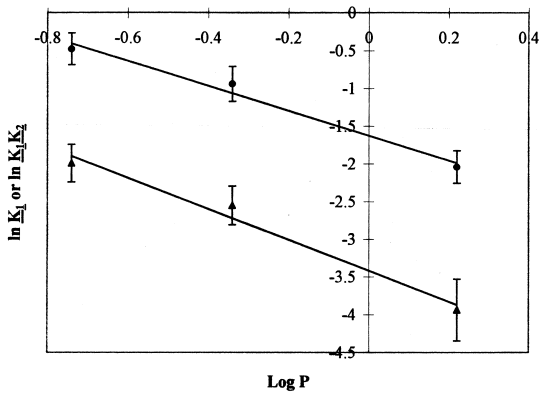

Fig. 10. Average $\ln \underline{K_1^m}$ (circles) and $\ln \underline{K_1^m K_2^m}$ (triangles) values against log P of the organic solvents in the mobile phase. Log P methanol $= -0.74$ [59], log P acetonitrile $= -0.34$ [59]. Log P THF $= 0.22$ [59]. The error bars are one standard deviation of the average.

standard deviations of the gA^m parameter estimates discussed next. A possible source of this error is from treatment of the solvation exchange constants as composition-independent parameters (as a first approximation). As was discussed earlier, such treatment assumes that the activity coefficients of all species in the solvation exchange scheme are invariant over the entire composition range which is unlikely.

3.1.2.2. The gA^m parameter

In earlier studies, Khossravi and Connors [22] applied a different version of the Phenomenological Model to solubility data of substituted biphenyls in methanol–water systems; they found that the gA term varied linearly with the non-polar surface area of the solutes by plotting gA against the non-polar surface area ($A_{nonpolar}$) of the various biphenyls. In later studies, LePree and coworkers [23] applied the Phenomenological Model to solubility data of naphthalene and 4-nitroaniline in various binary aqueous–organic solvent systems and found that the gA term is solvent dependent.

Similar to the solubility work, the gA^m parameter estimates are linearly dependent on the non-polar surface area of the solutes under investigation. This observation, which suggests the gA^m estimates are physically significant and predictable, is demonstrated in Fig. 11 where the gA^m parameter estimates are plotted against the non-polar surface area of the solute. Fig. 11 also demonstrates that the estimates are solvent-dependent as the slopes of the lines vary, and it provides a means to estimate values for the gA^m parameter.

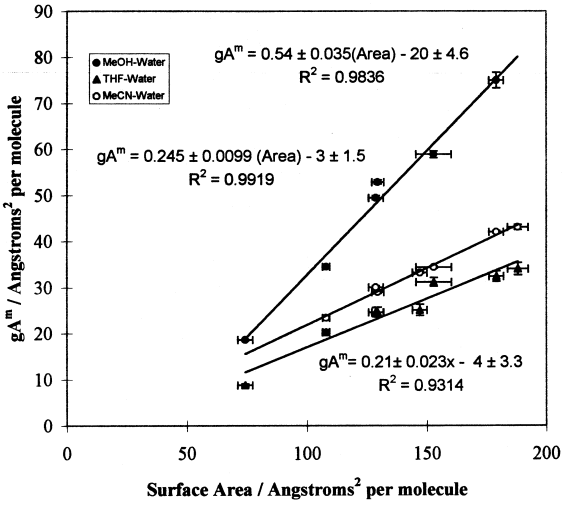

Fig. 11. gA^m estimates for anthracene, benzene, biphenyl, chlorobenzene, ethylbenzene, naphthalene, toluene, and phenol obtained from analysis of data from Schoenmakers and co-workers [57] against the non-polar surface area of these solutes.

4. Results and discussion – part two

4.1. One-step model – Eq. (23)

Data in Tables 1–4 were fit to the two-step model given by Eq. (22). While it was observed that the fits to the data were very good (as demonstrated by the values for r^2 and the curve fit criterion presented in Table 5), it was also observed that there were large errors in the parameter estimates, especially for 1-iodonapthalene. For example, the gA^m estimate was 120 ± 680 Å^2 per molecule. Note that the estimate for $\underline{K_2^m}$ for 1-iodonapthalene approaches zero; clearly, the model is too complex for this system. We applied the more simplistic one-step model [Eq. (23)] to our data and to the methanol–water data from Schoenmakers and co-workers [57] and discovered that the simple one-step model could adequately fit the data and more importantly, the parameter estimates still possess physical significance. It should be noted that although the one-step model appears to quantitatively describe all data for methanol–water mobile phases, it does not describe all data for acetonitrile–water and tetrahydrofuran systems; the fits to these data were poor or convergence to constant parameter estimates was unobtainable.

4.1.1. Curve fits

Figs. 12 and 13 show fits to our data (for benzene) and data from Schoenmakers and co-workers [57], respectively, and Table 7 shows r^2 and curve fit criterion values for the fits. The average value for the curve fit criterion for fits to the one-step model (with two adjustable parameters) is 0.884 ± 0.411 which is larger than the average value for the curve fit criterion for fits to the two-step model (0.46 ± 0.38) and indicates that slightly better fits are obtained with the more complicated two-step

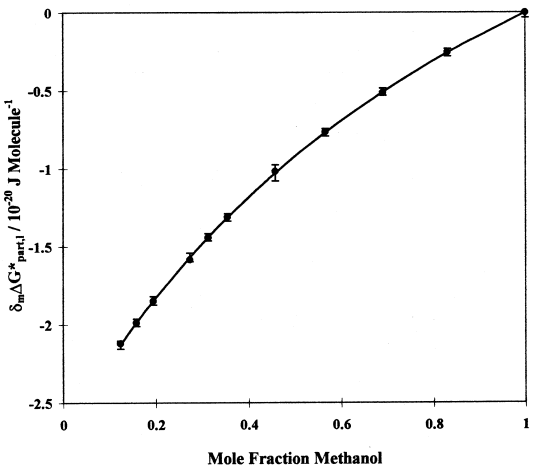

Fig. 12. Solvent effect on the retention of benzene in methanol–water binary cosolvent systems showing the experimental data points and the fitted curve for the one-step model [Eq. (23)]. The error bars are twice the standard deviation of $\delta_m\Delta G^*_{part,l}$.

model (with three adjustable parameters). However, the modest improvement in the fit to the data with the two-step model is outweighed by the greater precision in the parameter estimates obtained by using the one-step model and its greater simplicity.

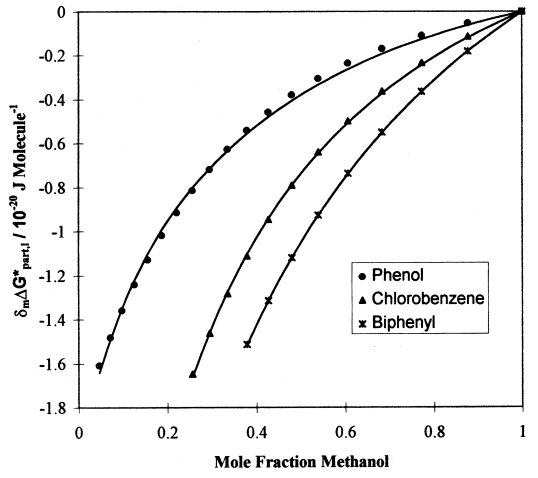

Fig. 13. Fits to data of various solutes in methanol–water binary cosolvent systems. (Data from Schoenmakers and coworkers [57]). The points are experimental, and the smooth curve is the fit of Eq. (23) to the data.

4.1.2. Parameter estimates

4.1.2.1. Solvation exchange constant

As with the two-step model, the solvation exchange constant is relatively independent of solute structure. The average value for the four solutes we examined is 0.41 ± 0.089, and the average value for the literature data is smaller and equal to 0.25 ± 0.061. The difference between the values becomes more apparent when the solvation exchange constant values for benzene are compared. The value for our study is 0.518 ± 0.0060 and that for literature data is 0.388 ± 0.0095. The lack of agreement in the solvation exchange constants could be attributable to differences in the columns used as Schoenmakers and coworkers used a silica-based C_{18} column while we employed a base-deactivated C_{18} column for our studies. However, more work is required to support this speculative argument.

4.1.2.2. The gA^m parameter

Similar to the gA^m parameter estimates obtained by fitting the data to the two-step model, the estimates obtained by fitting the data to the one-step model also vary with the molecular surface area of the solute. Fig. 14 is a plot of all the parameter estimates against the molecular surface areas of the solutes. It demonstrates that the estimates are linearly related to the surface areas; the equation of the line is $gA^m = 0.59\pm0.090$ (Area) -13 ± 12.6; $r^2 = 0.8422$. (The gA^m value for chlorobenzene is unusually high, if the regression is performed without this point, the equation of the line becomes $gA^m = 0.61\pm0.054$(Area) -17 ± 7.6; $r^2 = 0.9477$.) The plot is important because it suggests that the gA^m parameter estimates possess magnitudes of physical significance–they are proportional to the molecular surface areas of the solutes. It also demonstrates that the estimates are unique to the surface area of the molecule and the solvent used in the mobile phase, as the points from this study and from the literature fall on the same line even though they were obtained from analysis of chromatographic data collected under different temperatures, with different columns and with different flow-rates. (Recall that the Gibbs free energy for any process is dependent on temperature and pressure, and therefore, changes in flow-rate, which alter the pressure within the column, will

Table 7
Parameter Estimates Obtained by Fitting Eq. (23) to Data from Schoenmakers and Coworkers [57] and This Study

Solute	gA^m (S.D.)/Å^2 per molecule	Area (S.D.) /Å^2 per molecule	$\underline{K_1^m}$ (S.D.)	r^2 Curve fit[a]/%
Benzene	49.5 (0.16)	108 (1.5)	0.518 (0.0060)	0.9999
(This work)				0.656
Bromobenzene	65.9 (0.96)	144 (2.2)	0.42 (0.014)	0.9994
(This work)				1.59
Naphthalene	71.9 (0.91)	147 (3.0)	0.388 (0.0095)	0.9999
(This work)				0.768
1-Iodonaphthalene	98.0 (2.2)	188 (4.4)	0.303 (0.0099)	0.9998
(This work)				0.960
Benzene	40.7 (0.24)	108 (1.5)	0.355 (0.055)	0.9998
(Ref. [57])				1.046
Biphenyl	87.9 (0.39)	179 (3.0)	0.274 (0.016)	1.0000
(Ref. [57])				0.134
Chlorobenzene	84 (2.3)	129 (2.5)	0.178 (0.0062)	0.9998
(Ref. [57])				1.067
Ethylbenzene	76.6 (0.82)	153 (7.4)	0.250 (0.0038)	1.0000
(Ref. [57])				0.464
Phenol	27.9 (0.28)	74 (3.1)	0.234 (0.0065)	0.9987
(Ref. [57])				1.283
Toluene	72.4 (0.14)	129 (3.0)	0.207 (0.0055)	0.9999
(Ref. [57])				0.874

[a] Curve fit criterion = 100% × standard deviation about the fitted line/absolute value of the average of ordinate values.

affect $\Delta G^*_{part,l}$ unless the change in volume for the process is equal to zero.) This is extremely important because, according to the model, the gA^m estimates should only depend on the molecular surface area of the solute and the solvents in the mobile phase.

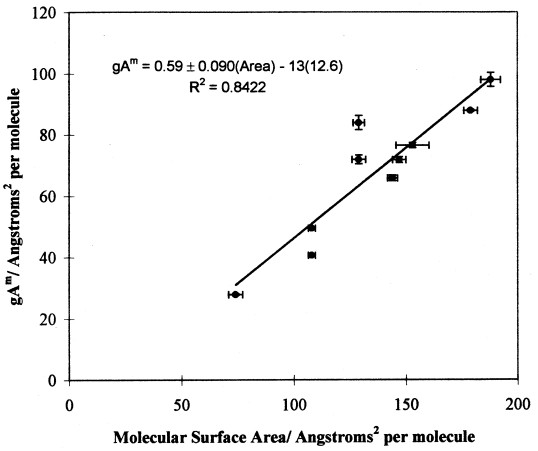

Fig. 14. gA^m parameter estimates for solutes from this study and from the study by Schoenmakers and co-workers [57] in methanol–water systems against their molecular surface areas.

4.2. Predictability

At this stage, much more work is needed before the model could be used to make a priori predictions of capacity factors. Specifically, we must increase our understanding of how the parameter estimates, particularly the solvation exchange constants, behave under different operating conditions. Furthermore, because we fit for a ratio of capacity factors, at least one experimental measurement must be made before other capacity factors could be calculated. Specifically, the capacity factor for the solute in a pure organic mobile phase must be measured, and we acknowledge that this is a difficult measurement to make for some poorly retained solutes. We did however decide to test the model's ability to make predictions of $\delta_m \Delta G^*_{part,l}$ by substituting estimates for gA^m, $\underline{K_1^m}$, and $\overline{K_1^m}$ that are obtained from the data in this paper. Eq. (22) was tested with data for the acetonitrile–

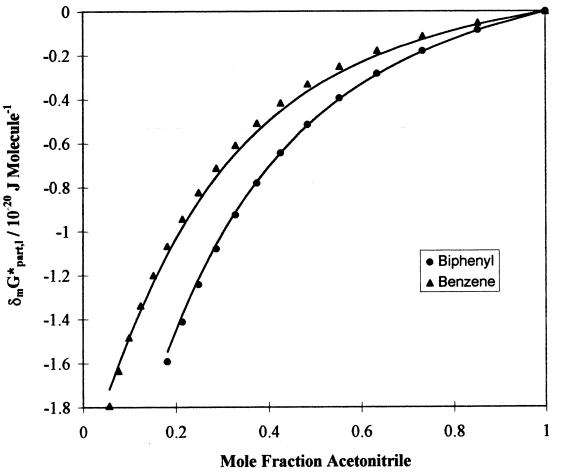

Fig. 15. Solvent effect on retention of various solutes in acetonitrile–water mobile phases. The data points are experimental, and the line is drawn with Eq. (22) and 'a priori' estimates for $\underline{K_1^m}$, $\underline{K_2^m}$ and gA^m obtained as described in Section 4.2.

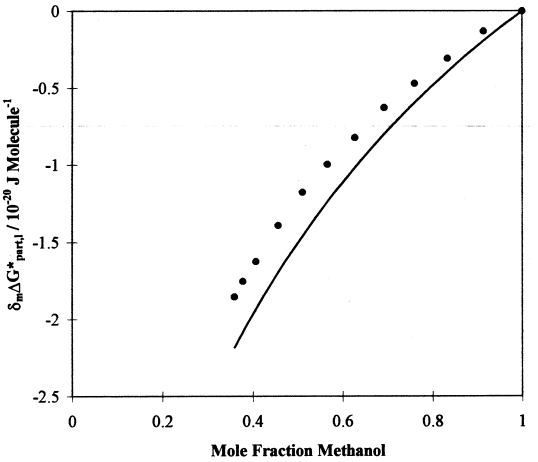

Fig. 17. Solvent effect on retention of 1-iodonaphthalene in methanol–water mobile phases. The data points are experimental, and the line is drawn with Eq. (23) and 'a priori' estimates for $\underline{K_1^m}$ and gA^m obtained as described in the Section 4.1.1.2.

water mobile phases by substituting average values for $\underline{K_1^m}$ and $\underline{K_2^m}$ ($\underline{K_1^m}=0.39$ and $\underline{K_2^m}=0.20$) and values for gA^m which were calculated from the linear equation in Fig. 11 and the surface area estimates in Table 6. Eq. (23) was tested with the methanol–water data from our laboratory. The average value for $\underline{K_1^m}$ ($\underline{K_1^m}=0.41$) reported earlier and values for gA^m, calculated from the linear equation in Fig. 14

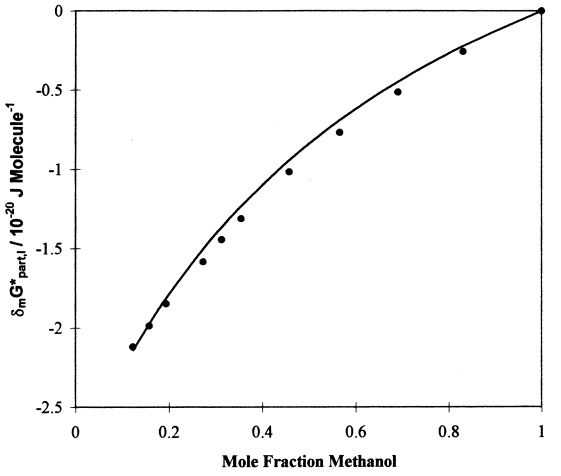

Fig. 16. Solvent effect on retention of benzene in methanol–water mobile phases. The data points are experimental, and the line is drawn with Eq. (23) and 'a priori' estimates for $\underline{K_1^m}$ and gA^m obtained as described in Section 4.2.

and the surface area estimates in Table 7, were substituted into Eq. (23). Mixed results were achieved. Data for benzene and biphenyl in acetonitrile–water mobile phases, shown in Fig. 15, are acceptably predicted. Data for benzene and 1-iodonapthalene in methanol–water are shown in Figs. 16 and 17, respectively. Although the fit for benzene is acceptable, that for 1-iodonapthalene is not. The cause of the inaccuracy is that the average value used $\underline{K_1^m}$ for differs greatly from the actual value for 1-iodonaphthalene while the estimated value for gA^m differs only slightly from the actual value.

5. Conclusions

The Phenomenological Model of solvent effects has been applied successfully, for the first time to retention data in RP-HPLC. The model could quantitatively relate retention to the composition of the mobile phase. It accounts for solvent–solvent interactions in the mobile and stationary phase through a cavity model and for solvent–solute interactions in these phases through a solvation exchange scheme. The parameter estimates, a curvature-corrected molecular surface area term and solvation exchange

constants, are obtained by fitting retention data to the model; they appear to be physically significant and potentially predictable.AcknowledgementsThe authors would like to thank Dr. Lloyd Synder, Dr. John G. Dorsey and especially Dr. Peter W. Carr for their helpful advice and comments concerning this manuscript.

Acknowledgements

The authors would like to thank Dr. Lloyd Synder, Dr. John G. Dorsey and especially Dr. Peter W. Carr for their helpful advice and comments concerning this manuscript.

References

[1] C.H. Lochmüller, C. Reese, A.J. Aschman, S.J. Breiner, J. Chromatogr. A 656 (1993) 3.
[2] K. Valkó, L.R. Synder, J.L. Glajch, J. Chromatogr. A 656 (1993) 501.
[3] L.R. Synder, J.W. Dolan, J.R. Gant, J. Chromatogr. 165 (1979) 3.
[4] B.P. Johnson, M.G. Khaledi, J.G. Dorsey, Anal. Chem. 58 (1986) 2354.
[5] J.J. Michels, J.G. Dorsey, J. Chromatogr. 457 (1988) 85.
[6] X. Geng, F.E. Regnier, J. Chromatogr. 332 (1985) 147.
[7] P. Jandera, J. Churácek, J. Chromatogr. 91 (1974) 207.
[8] R. Tijssen, H.A.H. Billiet, P.J. Schoenmakers, J. Chromatogr. 122 (1976) 185.
[9] P.J. Schoenmakers, H.A.H. Billiet, L. De Galan, J. Chromatogr. 282 (1983) 107.
[10] R. Tijssen, H.A.H. Billiet, P.J. Schoenmakers, J. Chromatogr. 128 (1976) 65.
[11] R. Tijssen, P.J. Schoenmakers, M.R. Böhmer, L.K. Koopal, H.A.H. Billiet, J. Chromatogr. A 656 (1993) 135–196.
[12] P.W. Carr, J. Li, A.J. Dallas, D.I. Eikens, L.C. Tan, J. Chromatogr. A 656 (1993) 113.
[13] O. Sinanoglu, in: J.O. Hirschfelder (Ed.), Advances in Chemical Physics, Vol. 12, Wiley, New York, 1967, p. 283.
[14] O. Sinananoglu, in: B. Pullman (Ed.), Molecular Associations in Biology, Academic Press, New York, 1968, p. 427.
[15] W. Melander, Cs. Horváth, I. Molnár, J. Chromatogr. 125 (1976) 129.
[16] Cs. Horváth, W.J. Melander, Chromatogr. Sci. 15 (1977) 393.
[17] K.A. Dill, J. Phys. Chem. 91 (1987) 1980.
[18] J.G. Dorsey, K.A. Dill, Chem. Rev. 89 (1989) 331.
[19] A. Vailaya, C. Horváth, J. Phys. Chem. B 101 (1997) 5875.
[20] K.B. Sentell, J. G Dorsey, Anal. Chem. 61 (1989) 930.
[21] D. Khossravi, K.A. Connors, J. Pharm. Sci. 81 (1992) 371.
[22] D. Khossravi, K.A. Connors, J. Pharm. Sci. 82 (1993) 817.
[23] J.M. LePree, M.J. Mulski, K.A. Connors, J. Chem. Soc. Perkin Trans. 2 (1994) 1491.
[24] D. Khossravi, K.A. Connors, J. Soln. Chem. 22 (1993) 321.
[25] K.A. Connors, M.J. Mulski, A. Paulson, J. Org. Chem. 57 (1992) 1794.
[26] K.A. Connors, D. Khossravi, J. Soln. Chem. 22 (1993) 677.
[27] M.J. Mulski, K.A. Connors, Supramol. Chem. 4 (1995) 271.
[28] R.D. Skwierczynski, K.A. Connors, J. Chem. Soc. Perkin Trans. 2 (1994) 467.
[29] J.M. LePree, K.A. Connors, J. Pharm. Sci. 85 (1996) 560.
[30] D. Khossravi, Ph.D. Thesis, University of Wisconsin–Madison, 1993.
[31] I.M. Klotz, in: Chemical Thermodynamics, Prentice-Hall, Inc. New York, 1950, p. 274–277.
[32] B.L. Karger, L.R. Synder, Cs. Horvath, in: An Introduction to Separation Science, John Wiley and Sons, New York, 1973, Ch 2.
[33] H. Maskill, in: The Physical Basis of Organic Chemistry, Oxford University Press, New York, 1993, p. 135.
[34] E.D. Katz, C.H. Lochüller, R.P.W. Scott, Anal. Chem. 61 (1989) 349.
[35] R.P.W. Scott, J. Chromatogr. A 656 (1993) 51.
[36] Y.C. Guillaume, C. Guinchard, Anal. Chem. 70 (1998) 608.
[37] W.P. Jencks, in: Catalysis in Chemistry and Enzymology, Dover Publications, Inc., New York, 1986, p. 433.
[38] C.A. Eckert, D.L. Bergman, D.L. Tomasko, M.P. Ekart Acc, Chem. Res. 26 (1993) 621.
[39] G.E. Berendsen, L. De Galan, J. Chromatogr. 196 (1980) 21.
[40] A. Tchapla, H. Colin, G. Guichon, Anal. Chem. 56 (1984) 621.
[41] A. Tchapla, S. Heron, J. Chromatogr. A 684 (1994) 175.
[42] L.C. Tan, P.W. Carr, J. Chromatogr. A 775 (1997) 1.
[43] P.W. Carr, L.C. Tan, J.H. Park, J. Chromatogr. A 724 (1996) 1.
[44] J.H. Park, Y.K. Lee, Y.C. Weon, L.C. Tan, J. Li, L. Li, J.F. Evans, P.W. Carr, J. Chromatogr. A 767 (1997) 1.
[45] R.M. McCormic, B.L. Karger, Anal. Chem. 52 (1980) 2249.
[46] R.M. McCormic, B.L. Karger, J. Chromatogr. 199 (1980) 259.
[47] C.R. Yonker, T.A. Zwier, M.F. Burke, J. Chromatogr. 241 (1982) 257.
[48] C.R. Yonker, T.A. Zwier, M.F. Burke, J. Chromatogr. 241 (1982) 269.
[49] P.W. Carr, J.M. Harris, Anal. Chem. 58 (1986) 626.
[50] P.W. Carr, J.M. Harris, Anal. Chem. 59 (1987) 2546.
[51] T.C. Schunk, M.F. Burke, J. Chromatogr. A 656 (1993) 289.
[52] E.H. Slatts, W. Markovski, J. Fekete, H. Poppe, J. Chromatogr. 207 (1981) 299.
[53] S.C. Rutan, J.M. Harris, J. Chromatogr. A 656 (1993) 197.
[54] J.G. Cole, J.G. Dorsey, Anal. Chem. 62 (1990) 16.
[55] Cs. Horvath, W. Melander, American Laboratory (1978) 17.
[56] H. Poppe, J. Chromatogr. A 656 (1993) 19.
[57] P.J. Schoenmakers, H.A.H. Billiet, L. De Galan, J. Chromatogr. 185 (1979) 179.
[58] R.D. Skwierczynski, K.A. Connors, J. Pharm. Sci. 83 (1994) 1690.
[59] A. Leo, C. Hansch, D. Elkins, Chem. Rev. 71 (1971) 525.